Electron Mobility Model for ⟨110⟩ Stressed Silicon Including Strain-Dependent Mass

Siddhartha Dhar, *Student Member, IEEE*, Enzo Ungersböck, Hans Kosina, *Member, IEEE*, Tibor Grasser, *Senior Member, IEEE*, and Siegfried Selberherr, *Fellow, IEEE*

***Abstract*—Stress-induced enhancement of electron mobility has primarily been attributed to the splitting of the conduction band minima. However, experiments have indicated that the mobility enhancement cannot solely be attributed to this effect, and a recent study has shown that stress along the ⟨110⟩ direction leads to a change of the effective mass. This work investigates the effect of the variation of the effective mass with stress along the ⟨110⟩ direction on the electron mobility. An improved low-field mobility model incorporating the effective mass change is presented.**

***Index Terms*—Effective mass, low-field mobility, mobility model, uniaxial stress/strain.**

I. Introduction

AGGRESSIVE scaling of device structures and the related performance gain in the last 20 years is increasingly difficult to be continued at the same pace. High mobility channel materials such as strained silicon with novel layout and device geometries are being increasingly sought after. In this regard the application of process-induced uniaxial stress along different channel directions seems to be technologically more promising and relevant than biaxial strain. Especially applying uniaxial stress along the ⟨110⟩ channel direction is beneficial for both electrons and holes. It has long been assumed that stress-induced enhancement of the electron mobility is due to the lifting of the degeneracy of the Δ_6 conduction band valleys with negligible change in the electron effective masses. However, experiments [1], [2] have indicated that the mobility enhancement cannot solely be attributed to the former effect, and a recent study has shown that a stress along the ⟨110⟩ direction leads to a change of the effective mass [3].

In this paper we present an improved low-field bulk electron mobility model for strained silicon. The model takes into account the effect of the variation of the effective mass with stress along the ⟨110⟩ direction on the electron mobility. Monte Carlo (MC) simulations were performed and the presented model is calibrated to the simulation results. The model is suitable for implementation in conventional device simulators.

II. Modeling

A. Strain Effects on Band Structure

The effect of stress on the band structure of silicon has been calculated using the empirical nonlocal pseudopotential method (EPM) [4]. For stress along the ⟨110⟩ direction, the effect of the internal displacement of the atoms [5], [6] has been taken into account in the band structure calculations. The effective masses for the twofold degenerate Δ_2-valleys and the fourfold degenerate Δ_4-valleys were extracted from the curvature of the energy bands at the conduction band minima.

B. Mobility Modeling

The mobility tensor for a stress along ⟨110⟩ can be calculated using the methodology proposed in [7]. The model in [7] calculates the electron mobility $\hat{\mu}^{(i)}_{\mathrm{n,str}}$ for the ith valley in strained silicon as a product of a scalar mobility and the scaled inverse mass tensor

$$\hat{\mu}^{(i)}_{\mathrm{n,str}}(N_I, \Delta\epsilon^{(i)}) = \frac{\beta \cdot \mu^L}{1+(\beta-1)\cdot h^{(i)}+\beta\cdot\left(\frac{\mu^L}{\mu^{LT}}-1\right)} \cdot \hat{m}^{-1}_{(i)}. \tag{1}$$

Here $\hat{m}^{-1}_{(i)}$ denotes the scaled effective mass tensor for the ith valley in silicon and $\beta = f \cdot m_t/m_c$. m_t and m_c denote the transversal and conductivity masses in silicon and f is an adjustable mobility enhancement factor. Details of the other variables used can be found in [7]. Equation (1) can be used to calculate the total mobility tensor for electrons in strained silicon as a function of doping concentration N_I and the strain-induced valley splitting $\Delta\epsilon^{(i)}$. The tensor in (1) is given in the principal coordinate system. The total mobility tensor is then computed by taking the weighted average of $\hat{\mu}^{(i)}_{\mathrm{n,str}}$ with the corresponding electron concentration $n^{(i)}_{\mathrm{str}}$ in the ith pair of valleys in strained silicon

$$\hat{\mu}^{\mathrm{tot}}_{\mathrm{n}} = \sum_{i=1}^{3} p^{(i)} \cdot \hat{\mu}^{(i)}_{\mathrm{n,str}} \tag{2}$$

$$p^{(i)} = \frac{n^{(i)}_{\mathrm{str}}}{\sum_{i=1}^{3} n^{(i)}_{\mathrm{str}}}$$

$$n^{(i)}_{\mathrm{str}} = N^{(i)}_C \cdot \exp\left[\frac{\Delta\epsilon^{(i)}}{k_B T}\right]. \tag{3}$$

1) Scalar Mobility: The scalar mobility depends on the strain-induced valley splitting $\Delta\epsilon$. From band structure calculations a shear deformation potential Ξ_u of 9.3 eV was extracted. This value can be used to calculate the strain-induced valley splitting for biaxially strained and uniaxially stressed silicon using linear deformation potential theory [8]. The components of the strain tensor needed to evaluate $\Delta\epsilon$ for the case of uniaxial stress of magnitude P applied along a general direction can be obtained as follows.

We adopt a coordinate system (x', y', z') in which the stress tensor has only one nonzero component $\sigma'_{xx} = P$. This system

Manuscript received June 10, 2006; revised August 18, 2006. This work was supported in part by the European Commission under Project D-DOT FET 012150-2. The review of this paper was arranged by Associate Editor R. Lake.

The authors are with Institute for Microelectronics, Technische Universität Wien, A-1040 Vienna, Austria (e-mail: dhar@iue.tuwien.ac.at).

Digital Object Identifier 10.1109/TNANO.2006.888533

1536-125X/$25.00 © 2007 IEEE

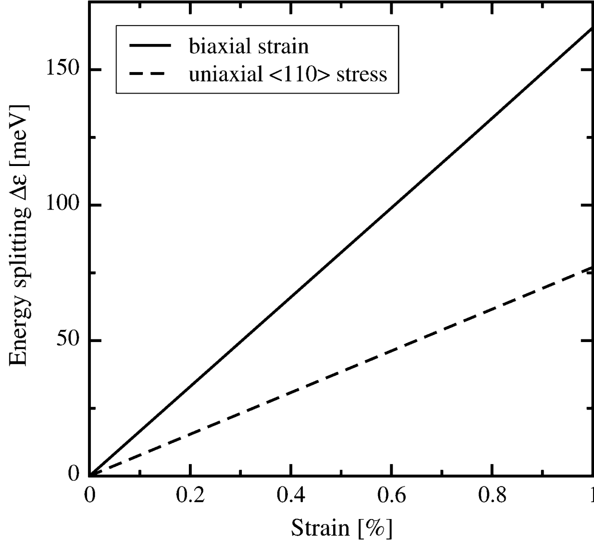

Fig. 1. Effect of biaxial tensile strain and uniaxial $\langle 110 \rangle$ tensile stress on valley splitting. The strain component in the stressed direction is plotted.

is related to the coordinate system (x, y, z) of the primary crystallographic axes of the semiconductor by a rotation $\bar{U}$

$$\bar{U}(\theta, \phi) = \begin{pmatrix} \cos\theta\cos\phi & -\sin\phi & \sin\theta\cos\phi \\ \cos\theta\sin\phi & \cos\phi & \sin\theta\sin\phi \\ -\sin\theta & 0 & \cos\theta \end{pmatrix}. \quad (4)$$

The angles θ and ϕ are the polar and azimuthal angles of the stress direction relative to the coordinate system (x, y, z). Using the relationship between coordinate systems for tensors, the stress in the principal system can be calculated from

$$\sigma_{ij} = U_{\alpha i} U_{\beta j} \sigma'_{\alpha\beta}. \quad (5)$$

The strain components can be calculated by inversion of Hook's law $\varepsilon_{ij} = S_{ijkl}\sigma_{kl}$, where S_{ijkl} denotes the elastic compliance tensor and ε_{ij} the strain tensor. Using the above relations the strain for uniaxial stress of magnitude P applied along [110] reads in the principal coordinate system as

$$\bar{\varepsilon}_{[110]} = \begin{pmatrix} (s_{11}+s_{12})P/2 & s_{44}P/4 & 0 \\ s_{44}P/4 & (s_{11}+s_{12})P/2 & 0 \\ 0 & 0 & s_{12}P \end{pmatrix}. \quad (6)$$

Here, s_{11}, s_{12}, and s_{44} are the three independent compliance constants of a semiconductor with cubic symmetry. Strain from stress in general directions $[hkl]$ can be obtained by applying the proper coordinate transformation in (4). Fig. 1 shows the splitting, $\Delta\epsilon$ for biaxially strained and uniaxially stressed silicon. It is observed that biaxial tension is more effective in splitting the conduction band valleys than $\langle 110 \rangle$ uniaxial tension.

2) Effective Mass Variation: The model in [7] assumes constant values for m_t and m_l in silicon. Band structure calculations show that for a uniaxial tensile stress along $\langle 110 \rangle$, the twofold degenerate Δ_2-valleys which are lowered in energy, experience a change in the effective masses. Fig. 2 depicts the variation of the in-plane masses parallel $(m_{t\|})$ and perpendicular $(m_{t\perp})$ to the stress, and the longitudinal (m_l) masses for the Δ_2-valleys as a function of the strain for different values of the internal displacement parameter ξ. It can be seen that there is a significant change in Δm^* for increasing strain along $\langle 110 \rangle$.

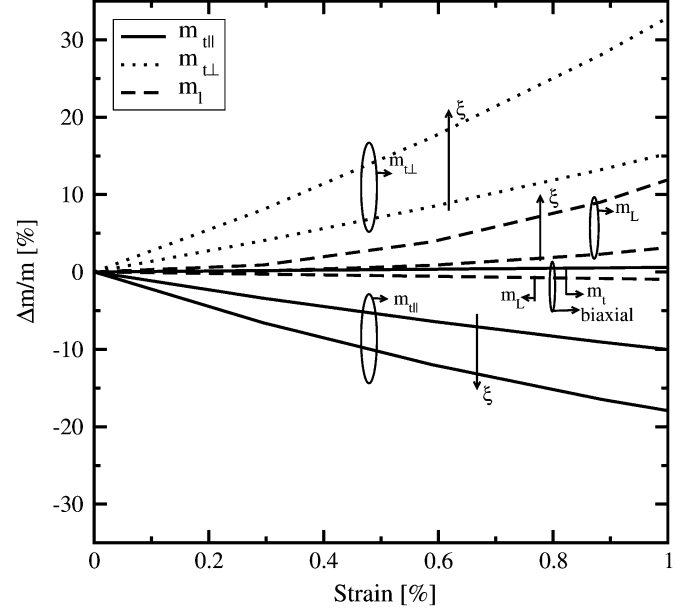

Fig. 2. Effect of uniaxial $\langle 110 \rangle$ and biaxial tensile strain on the transversal and longitudinal masses of the Δ_2-valleys in silicon for two different values of internal strain parameter ($\xi = 0.0$ and 1.0).

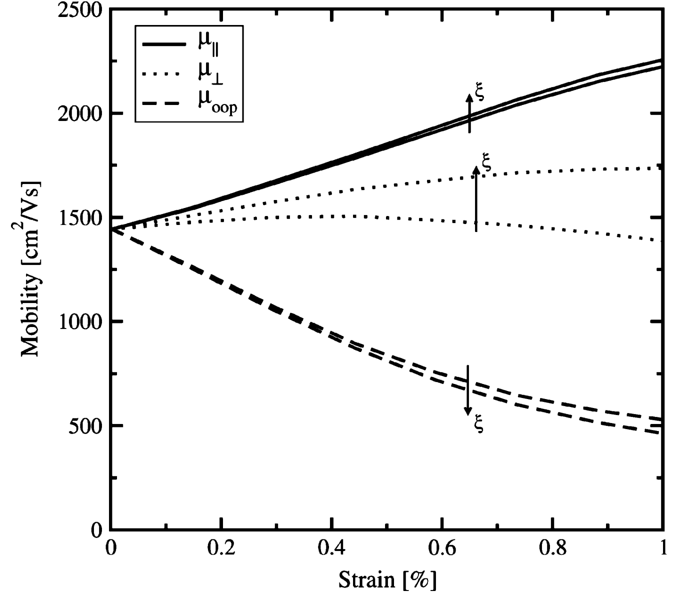

Fig. 3. Parallel $(\mu_{\|})$, perpendicular $(\mu_{\perp})$, and out-of-plane (μ_{oop}) mobility components as a function of tensile strain along [110] direction for two different values of internal displacement parameter ($\xi = 0$ and 1.0).

This variation of the effective masses has been parameterized using

$$\begin{aligned} m_{t\|} &= 0.196 - 0.016 \cdot P \\ m_{t\perp} &= 0.196 + 0.029 \cdot P \\ m_l &= 0.918 + 0.0236 \cdot P^2. \end{aligned} \quad (7)$$

Here P denotes the magnitude of uniaxial tensile stress along $\langle 110 \rangle$ in units of GPa. Fig. 3 shows how the variation of the effective masses translates into a mobility variation. The mobilities in Fig. 3 were calculated using MC simulations [9] taking into account the effective mass changes. An efficient zero-field algorithm [10] has been employed in the MC simulations for es-

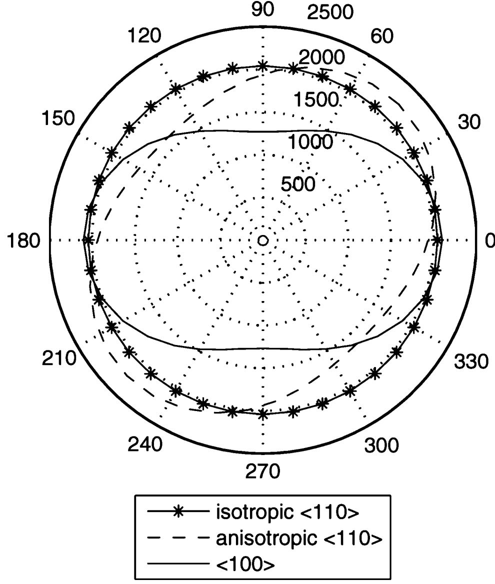

Fig. 4. Variation of the in-plane mobility with in-plane angle for 1.5 GPa uniaxial ⟨100⟩ and ⟨110⟩ tensile stress.—⋆: ⟨110⟩ without mass correction;——: ⟨110⟩ with mass correction;—: 1.5 GPa uniaxial tensile ⟨100⟩ stress.

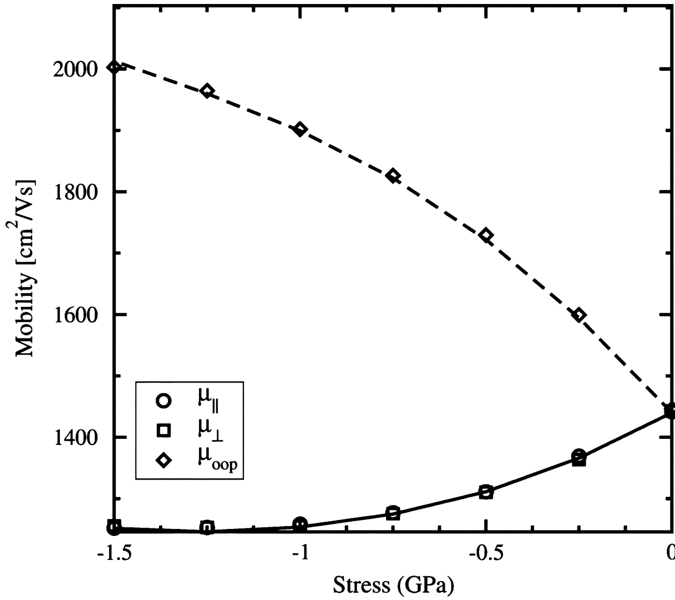

Fig. 5. Comparison of parallel ($\mu_{\|}$), perpendicular ($\mu_{\perp}$), and out-of-plane (μ_{oop}) electron mobility components obtained from the MC simulations (symbols) and the analytical model (lines) for uniaxial ⟨110⟩ compressively strained silicon. Here $m_{t\|} = m_{t\perp}$.

timating the low-field mobilities. As can be seen from the figure, the direction of stress leads to a pronounced anisotropy of the mobility in the transport plane. In Fig. 4 the anisotropy of the mobility is compared for ⟨110⟩ and ⟨100⟩ stress directions with and without the change in effective masses. The internal strain parameter ξ was set to 0.53 according to the theoretical calculations [11]. It can be clearly seen from the figure that Δm_t cannot be neglected for ⟨110⟩ uniaxial stress. For uniaxial compression, however, there is a negligible change in the effective masses of the lowered fourfold degenerate Δ_4-valleys.

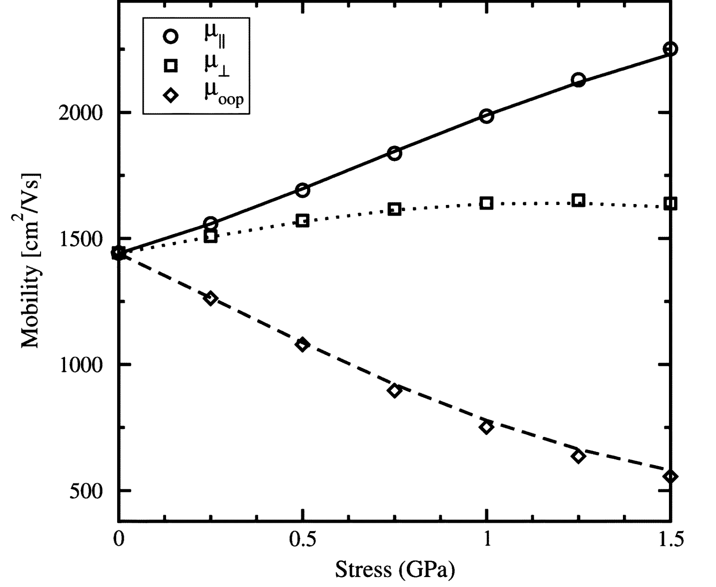

Fig. 6. Comparison of parallel ($\mu_{\|}$), perpendicular ($\mu_{\perp}$), and out-of-plane (μ_{oop}) electron mobility components obtained from the MC simulations (symbols) and the analytical model (lines) for uniaxial ⟨110⟩ tensile strained silicon.

3) Inverse Mass Tensor: The model in [7] has been extended to account for the variation of the effective mass of the Δ_2-valleys with uniaxial tensile stress. Consider the energy dispersion relation for stress along the $[110]$ direction

$$\epsilon(k) = \frac{\hbar^2}{2}\left(\frac{k_{[110]}^2}{m_{t\|}} + \frac{k_{[\bar{1}10]}^2}{m_{t\perp}} + \frac{k_z^2}{m_l}\right). \tag{8}$$

The wave vectors k_{110} and $k_{[\bar{1}10]}$ can be expressed in terms of wave vectors in the principal coordinate (x, y, and z) system as

$$k_{110} = \frac{(k_x + k_y)}{\sqrt{2}} \quad k_{[\bar{1}10]} = \frac{(k_x - k_y)}{\sqrt{2}}. \tag{9}$$

Substituting (9) into (8) yields

$$\begin{aligned}\epsilon(k) = &\frac{\hbar^2}{2}\left(k_x^2\left[\frac{1}{m_{t\|}} + \frac{1}{m_{t\perp}}\right] + k_y^2\left[\frac{1}{m_{t\|}} + \frac{1}{m_{t\perp}}\right]\right)\\ &+ \frac{\hbar^2}{2}\left(2k_xk_y\frac{1}{2}\left[\frac{1}{m_{t\|}} - \frac{1}{m_{t\perp}}\right] + \frac{k_z^2}{m_l}\right).\end{aligned} \tag{10}$$

From (10) the scaled inverse mass tensor can be found

$$\hat{m}_z^{-1} = m_c \begin{pmatrix} m_t^{-1} & m_\Delta^{-1} & 0 \\ m_\Delta^{-1} & m_t^{-1} & 0 \\ 0 & 0 & m_l^{-1} \end{pmatrix} \tag{11}$$

$$m_t^{-1} = (m_{t\|}^{-1} + m_{t\perp}^{-1})/2$$

$$m_\Delta^{-1} = (m_{t\|}^{-1} - m_{t\perp}^{-1})/2) \tag{12}$$

$$m_c^{-1} = (m_{t\|}^{-1} + m_{t\perp}^{-1} + m_l^{-1})/3. \tag{13}$$

The mobility tensor in (1) calculated using $\hat{m}_z^{-1}$ thus becomes nondiagonal in the principal coordinate system. The mobility along the two in-plane ([110] and [$\bar{1}$10]) and perpendicular ([001]) directions is obtained by taking a projection of the total mobility tensor (2) in the direction of the in-plane and perpendicular vectors. Fig. 5 shows a comparison of the variation of

the electron mobility components with increasing compressive stress as obtained from MC simulations and the analytical model. Since the effective masses do not change under compressive stress, two components of mobility are identical. Three different components of the mobility appear for the case when uniaxial tensile stress is applied along the [110] direction. This can be seen in Fig. 6. Our model shows good agreement with the MC simulation results.

III. Conclusion

It can be concluded that the mobility enhancement does not arise solely from strain-induced valley splitting but also from the variation in the effective masses. An improved analytical model has been presented to describe the anisotropy of the electron mobility in $\langle 110 \rangle$ stressed silicon. The model includes the variation of the effective masses with stress as well as the effect of reduction of intervalley scattering due to valley splitting, and doping and temperature dependence. Results obtained from the model show excellent agreement with MC simulations. The model is appropriate for implementation in TCAD simulators.

References

[1] K. Uchida, R. Zednik, C. Lu, H. Jagannathan, J. McVittie, P. McIntyre, and Y. Nishi, "Experimental study of biaxial and uniaxial strain effects on carrier mobility in bulk and ultrathin-body SOI MOSFETs," in *IEDM Tech. Dig.*, 2004, pp. 229–232.

[2] H. Irie, K. Kita, K. Kyuno, and A. Toriwni, "In-plane mobility anisotropy and universality under uni-axial strains in N- and P-MOS inversion layers on (100), (110), and (111) Si," in *IEDM Tech. Dig.*, 2004, pp. 225–228.

[3] K. Uchida, T. Krishnamohan, K. C. Saraswat, and Y. Nishi, "Physical mechanisms of electron mobility enhancement in uniaxial stressed MOSFETs and impact of uniaxial stress engineering in ballistic regime," in *IEDM Tech. Dig.*, 2005, pp. 135–138.

[4] M. Rieger and P. Vogl, "Electronic-band parameters in strained $Si_{1-x}Ge_x$ alloys on $Si_{1-y}Ge_y$ substrates," *Phys. Rev. B*, vol. 48, no. 19, pp. 14 276–14 287, 1993.

[5] E. Ungersboeck, S. Dhar, G. Karlowatz, H. Kosina, and S. Selberherr, "Physical modeling of electron mobility enhancement for arbitrarily strained silicon," in *11th Int. Workshop on Computational Elecronics, Book of Abstracts*, 2006, pp. 141–142.

[6] C. G. V. de Walle, "Theoretical calculations of heterojunction discontinuities in the Si/Ge system," *Phys. Rev. B*, vol. 34, no. 8, pp. 5621–5633, 1986.

[7] S. Dhar, H. Kosina, V. Palankovski, E. Ungersboeck, and S. Selberherr, "Electron mobility model for strained-Si devices," *IEEE Trans. Electron Devices*, vol. 52, no. 4, pp. 527–533, Apr. 2005.

[8] I. Balslev, "Influence of uniaxial stress on the indirect absorption edge in silicon ansiliconrmanium," *Phys. Rev.*, vol. 143, pp. 636–647, 1966.

[9] Institut für Mikroelektronik, Technische Universität Wien, Wien, Austria, *VMC 2.0 User's Guide,* 2006 [Online]. Available: http://www.iue.tuwien.ac.at/software

[10] S. Smirnov, H. Kosina, M. Nedjalkov, and S. Selberherr, "A zero field Monte Carlo algorithm accounting for the pauli exclusion principle," in *Proc. 4th Int. Conf. Large-Scale Scientific Computing*, 2003, pp. 185–193.

[11] O. Nielson and R. Martin, "Stresses in semiconductors: Ab initio calculations on Si, Ge, and GaAs," *Phys. Rev. B*, vol. 32, no. 6, pp. 3792–3805, 1985.

Siddhartha Dhar (S'06) was born in New Delhi, India, in 1979. He received the B.E. degree in electrical engineering from the Delhi College of Engineering, India in 2001 and the M.Sc. degree in microelectronics and microsystems from the Technical University of Hamburg-Harburg, Germany, in 2003. He is currently working toward the Ph.D. degree from the Institute for Microelectronics at the Technische Universität Wien, Vienna, Austria.

His research interests include device modeling and simulation of strained Si CMOS transistors and circuit level simulation in general.

Enzo Ungersböck was born in Vienna, Austria, in 1977. He received the Diplomingenieur degree from the Technische Universität Wien, Vienna, Austria, in 2002. He is currently working toward the Ph.D. degree from the Institute for Microelectronics at the Technische Universität Wien.

He held a visiting research position at the Samsung Advanced Institute of Technology in Seoul, Korea, in Summer 2003. His scientific interests include Monte Carlo simulation, band structure calculations, simulation of carbon nanotubes, and quantum mechanical confinement in submicrometer MOSFETs.

Hans Kosina (S'89–M'93) received the Diplomingenieur degree in electrical engineering, the Ph.D. degree, and the *venia docendi* in microelectronics from the Technische Universität Wien, Vienna, Austria, in 1987, 1992, and 1998, respectively.

He was for one year with the Institute of Flexible Automation, Technische Universität Wien, and joined then the Institute for Microelectronics, where he is currently an Associate Professor. In summer 1993 he was a Visiting Scientist at Motorola Inc., Austin, TX, and in summer 1999 a Member of Visiting Faculty at Intel Corp., Santa Clara, CA. His current research interests include device modeling of semiconductor devices, nanoelectronic devices, organic semiconductors and optoelectronic devices, development of novel Monte Carlo algorithms for classical and quantum transport problems, and computer aided engineering in ULSI technology.

Dr. Kosina is Associate Editor of the IEEE Transactions on Computer-Aided Design of Circuits and Systems since January 2004.

Tibor Grasser (SM'05) was born in Vienna, Austria, in 1970. He received the Diplomingenieur degree in communications engineering, the Ph.D. degree in technical sciences, and the *venia docendi* in microelectronics from the Technische Universität Wien, Vienna, in 1995, 1999, and 2002, respectively.

He joined the Institute for Microelectronics, Technische Universität Wien, in 1996, where he is currently employed as an Associate Professor. Since 1997, he has headed the MINIMOS-NT development group, working on the successor of the highly successful MINIMOS program. From October to December 1997, he was with Hitachi Ltd., Tokyo, Japan, as a Visiting Research Engineer. In 2001 he was also a Visiting Researcher in the Alpha Development Group, Compaq Computer Corporation, Shrewsbury, NJ. In 2003, he was appointed Head of the Christian Doppler Laboratory for TCAD in Microelectronics, an industry-funded research group embedded in the Institute for Microelectronics. His current scientific interests include circuit and device simulation, device modeling, and reliability issues.

Siegfried Selberherr (M'79–SM'84–F'93) was born in Klosterneuburg, Austria, in 1955. He received the Diplomingenieur degree in electrical engineering, the Ph.D. degree in technical sciences, and the *venia docendi* in computer-aided design from the Technische Universität Wien, Vienna, Austria, in 1978, 1981, and 1984, respectively.

Since 1988 he has been the Chair Professor of the Institute for Microelectronics and from 1999 to 2005 served as Dean of the Fakultät für Elektrotechnik und Informationstechnik at the Technische Universität Wien. His current research interests are modeling and simulation of problems for microelectronics engineering.